

Preparation of Aqueous Soluble Polyamides from Renewable Succinic Acid and Citric Acid as a New Approach to Design Bio-inspired Polymers

Man Jiang,^{1,2,3} Guangsong Chen,² Ping Lu,^{2,3} Jian Dong^{1,2,3}

¹Faculty of Materials Science and Chemical Engineering, Ningbo University, Ningbo, Zhejiang Province 315211, China

²School of Chemistry and Chemical Engineering, Shaoxing University, Shaoxing, Zhejiang Province 312000, China

³Zhejiang Provincial Key Laboratory of Alternative Technologies for Fine Chemicals, Shaoxing, Zhejiang Province 312000, China

Correspondence to: J. Dong (E-mail: jiangdong@usx.edu.cn)

ABSTRACT: A novel type of aqueous soluble polyamides were prepared as renewable substitutes for ecologically benign poly(aspartic acid) by polymerization of succinic acid ester and hexamethylene diamine in the presence of citric acid ester. The copolymerization resulted in the formation of poly(amide imide) intermediates, which were hydrolyzed to aqueous solutions of polyamides. The hydrolyzed products were confirmed to be copolymers of succinamide and citramide with COOH side chains, similar to poly(aspartic acid). The polyamides showed strong chelating abilities to Ca^{2+} and Pb^{2+} metals, comparable to poly(aspartic acid). Interestingly, they also demonstrated antifreeze activities in water by reducing the ice fractions. The polyamides represent a new class of metal chelators and antifreeze protein mimics derived from succinamide and citramide. © 2013 Wiley Periodicals, Inc. *J. Appl. Polym. Sci.* **2014**, *131*, 39807.

KEYWORDS: polyamides; biopolymers and renewable polymers; polycondensation; hydrophilic polymers

Received 30 January 2013; accepted 27 July 2013

DOI: 10.1002/app.39807

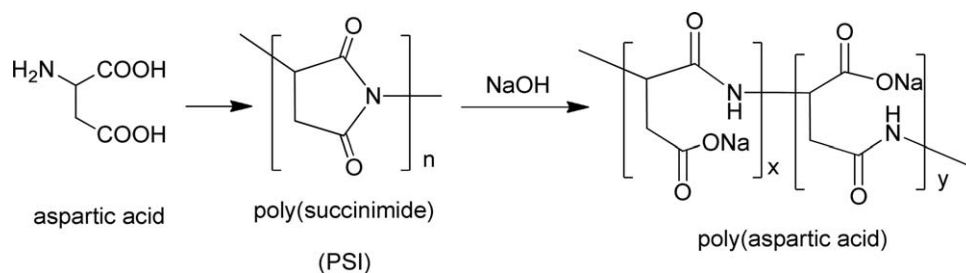
INTRODUCTION

Aqueous soluble polyamides can be structurally designed and used as proteinaceous materials to mimic natural proteins and provide unique cryoprotection for living cells, biologically active substances and food, as natural antifreeze proteins do.^{1,2} In addition, they have played important roles in metal chelation, ion exchange, drug delivery, fiber modification and inhibition of gas hydrate crystal growth in deep sea drilling.^{3–8} For preparation of water soluble polyamides, several methods can be used: (a) polycondensation of amino acids to form polypeptides and polyamides^{9–13}; (b) polymerization between certain hydrophilic diacids (or acid derivatives) and diamines^{14–18}; and (c) enzymatic production of certain poly(amino acid)s by bacteria.^{9,19–21}

Among the water-soluble polyamides, poly(aspartic acid)s (PASPs) have been recognized as eco-friendly water-soluble synthetic poly(amino acid)s and used as dispersants, metal chelators, detergent builders, and in biomedical applications. PASPs also possess antifreeze properties by reducing ice fractions in water.¹⁹ At present, PASPs are prepared by thermal polycondensation of aspartic acid to poly(succinimide) (PSI) intermediate and subsequent hydrolysis of PSI, as shown in

Scheme 1 for the synthetic approach. Recently, poly(tartaramide)s, prepared from L-tartaric acid, have been shown to function as artificial antifreeze polymers which strongly interfere with the crystallization of water.²² Poly(aspartamide)s, another polymer with a peptide backbone structure prepared by reaction between alkylamines and poly(succinimide)s, have also been tested as gas hydrate crystal inhibitors.²³ Poly(aspartamide)s also exhibit good seawater biodegradability. Because the aspartic acid is now made from plant sources, PASPs and poly(aspartamide)s are renewable resource-based materials. They have also been shown to protect against calcium carbonate or barium sulfate scale formation in oilfields.^{24–27} PASP and aspartic acid oligomers resemble functional domains of aspartic acid-rich proteins and provide valuable models for understanding how these proteins regulate mineralization in nature or *in vivo*.^{1,2}

In this study, we report preparation of water soluble polyamides based on succinic acid and citric acid in a method partially analogous to synthesis of PASPs (Scheme 1) but different from the latter in the raw materials used. The process is carried out by copolymerizing with citric acid ester to form



Scheme 1. Conventional synthesis of poly(aspartic acid).

poly(succinimide) segments in the main chain and subsequent hydrolysis (Scheme 2). The obtained succinamide-citramide copolymers show strong chelating ability to Ca^{2+} and Pb^{2+} metals, which is comparable to PASP. The polyamides also demonstrate antifreeze activities as effective as well-known antifreeze materials such as glucose and poly(amino acid)s. In industry, both succinic acid and citric are mass-produced by fermentation from agricultural products such as starch.^{28–30} Therefore, the polyamides prepared here are renewable alternatives to PASPs or nonbiodegradable chelators such as poly(acrylic acid).

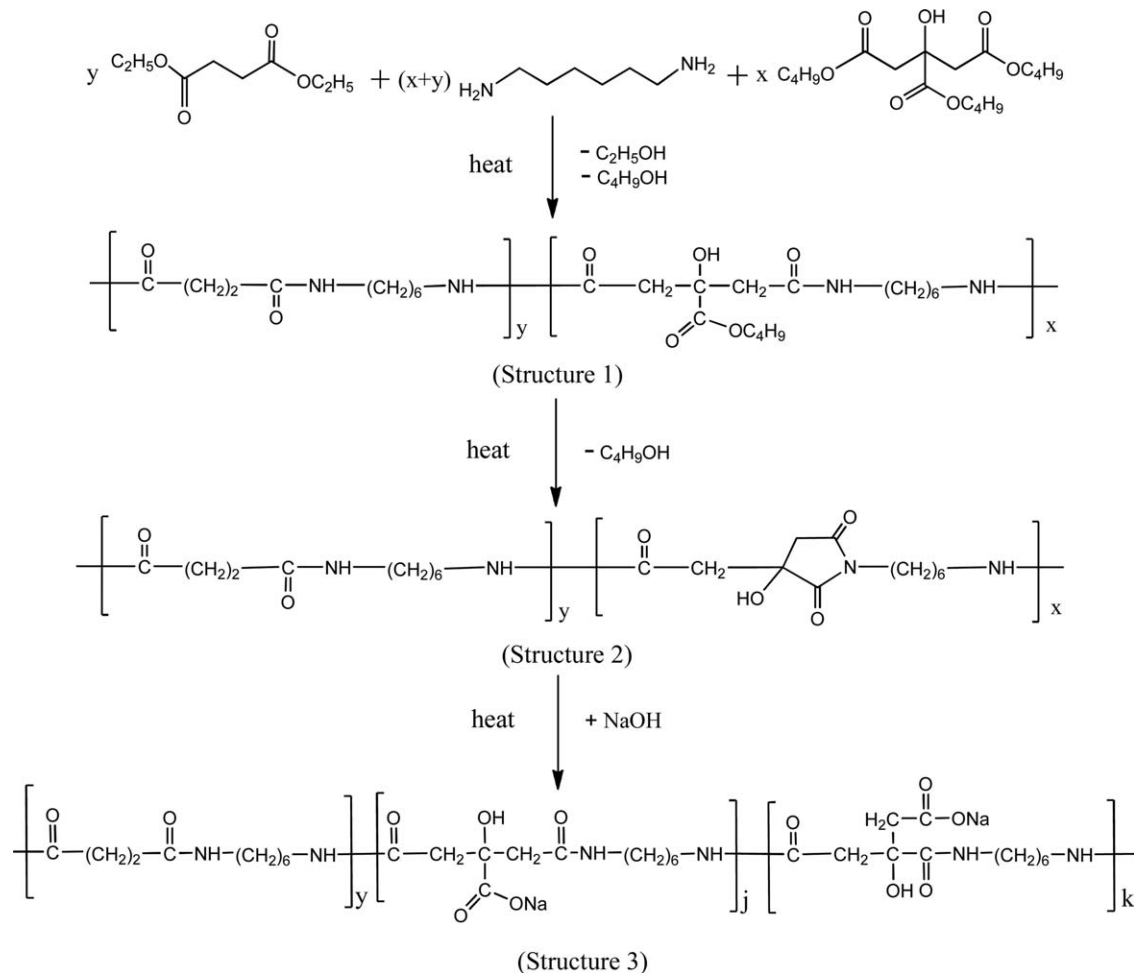
EXPERIMENTAL

Materials

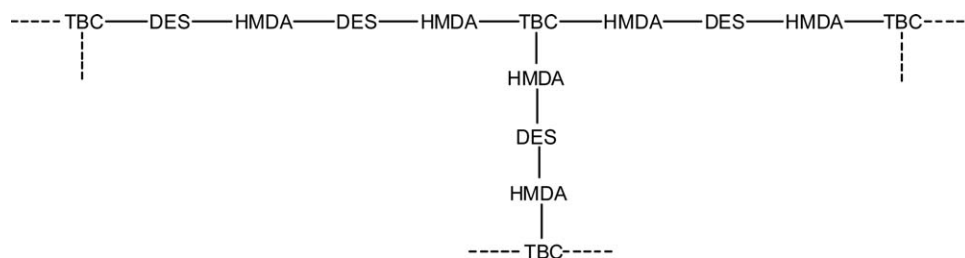
Diethyl succinate (DES), tributyl citrate (TBC), and hexamethylenediamine (HMDA), ethanol, and acetone, all in analytical grade, were purchased from Sinopharm.

Preparation of Water-Soluble Polyamides

Polyamides were first prepared from DES and HMDA at an equimolar ratio of $y(\text{DES}) : z(\text{HMDA}) = 1 : 1$. Copolymers of DES and TBC with HMDA were prepared at equal molar ratios of total esters and HMDA, namely, $[x(\text{TBC}) + y(\text{DES})]$:



Scheme 2. Copolymerization of diethyl succinate and hexamethylenediamine with tributyl citrate and hydrolysis products.



Scheme 3. Branched structure of the polyamide formed from Structure 1 in Scheme 2.

$z(\text{HMDA}) = 1 : 1$, with $x(\text{TBC}):y(\text{DES}) = 1 : 2, 3 : 2$, or $3 : 1$, respectively, giving poly(amide imide)s with variable imide contents.

In a typical experiment, 17.2 mmol of TBC, 34.4 mmol of DES, and 51.6 mmol of HMDA were mixed in a 250-mL round bottom flask, and heated at 60°C in a vacuum evaporator for 6 h. The mixtures were cast evenly in 10 cm × 10 cm TEFLON molds, forming white films in 24 h. The prepolymer films were heated in a vacuum oven at 70°C for 12 h, then at 160°C for 4 h, and finally at 200°C for 4 h, resulting in red strong films. Nearly 2 g of these films were heated in a NaOH solution (pH = 14) at 80°C for 8 h, until the samples were totally dissolved, yielding a light yellow clear solution. The polymer solution was evaporated in a vacuum evaporator, and the resulting solid was dried in a vacuum oven at 60°C for 12 h. The powdered products were dissolved in water, precipitated in large amount of ethyl alcohol, and isolated by centrifugation. The obtained precipitates were finally dried in vacuum.

Characterization

FTIR spectra were recorded at 4 cm⁻¹ resolution on a Nicolet 6700 FTIR spectrometer (Thermo Fisher Scientific). Dynamic mechanical analysis (DMA) was performed with a heating rate of 3°C min⁻¹ in tension mode at mechanical frequencies of 1.0, 10.0, 30.0 Hz by using a DMA 8000 dynamic mechanical analyzer (Perkin Elmer). The samples were cut in a size of 10 mm × 3 mm × 0.5 mm. Wide-angle X-ray diffraction analysis was performed on an X-ray diffractometer (PANalytical B.V., Model Empyrean) using Ni-filtered Cu K α radiation (40 kV, 250 mA), $\lambda = 1.5418 \text{ \AA}$, in a scanning range of $2\theta = 3^\circ\text{--}90^\circ$, with a step size of 0.026° and a scanning rate of 5° min⁻¹. Tensile tests of the films were prepared by cutting dumbbell-shaped samples and measured at a stretching rate of 50 mm min⁻¹ according to ASTM D638-10, by using a universal tensile test machine (Model CMT 6104, SANS). Three to four

parallel samples were made in the tensile test and the data were averaged.

¹H and ¹³C NMR spectra were collected in D₂O solutions by using a Bruker AVANCE III 400 MHz NMR spectrometer. Sample concentrations of about 5 and 10% (w/v) were used for the ¹H and ¹³C analyses, respectively. Two-dimensional (2D) ¹H-¹³C-heteronuclear single quantum coherence (¹H-¹³C-HSQC) spectra were collected with a Bruker pulse sequence (HSQCETGP). The weight-average molecular weights (M_w) and number-average molecular weights (M_n) were measured by aqueous GPC (Agilent 1100 GPC system) relative to narrow distribution polystyrene sodium sulfonate standards and Pullulan standards on a PL aquagel-OH 8 μm MIXED-H column (300 × 7.5 mm²), using a water mobile phase, a flow rate of 1.0 mL min⁻¹ and a refractive index detector. Differential scanning calorimetric analysis was conducted on Diamond DSC instrument (Perkin Elmer).

The calcium and lead ion chelating capabilities of the obtained polyamides were determined using a Ca²⁺- and a Pb²⁺- selective electrode, respectively, and an ion meter according to the procedures described in previous studies.^{31–33} Briefly, a sample (10.0 mg) was dissolved in 50 mL of a pH = 7.0 aqueous solution, which had been adjusted to give a CaCl₂ concentration of 1.0 mmol L⁻¹ (or a PbNO₃ concentration of 1.0 mmol L⁻¹) and a KCl concentration of 0.08 mol L⁻¹. The resulting mixture was stirred at 30°C for 10 min and the Ca²⁺ ions

Table I. Critical Extent of Reaction (p_c) of Succinamide-Citramide Copolymers

Sample	Ratio			r	ρ	p_c
	TBC	DES	HMDA			
1	1	2	3	1.5	0.43	0.68
2	3	2	5	2.5	0.69	0.49
3	3	1	4	4.0	0.82	0.37

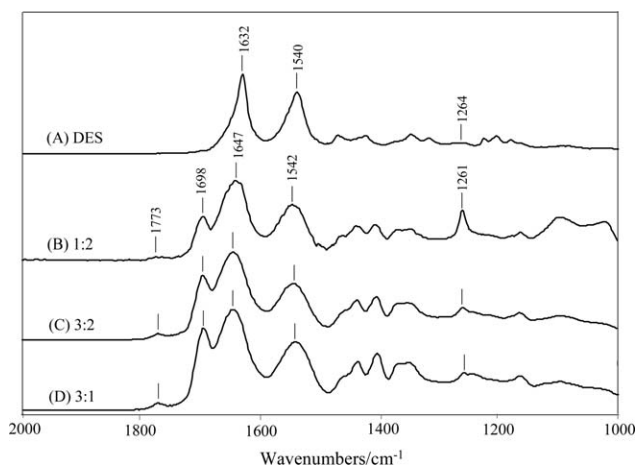


Figure 1. FTIR spectra of polymers formed between HMDA and different esters: (A) pure DES; (B) mixture of $x(\text{TBC}):y(\text{DES}) = 1 : 2$; (C) mixture of $x(\text{TBC}):y(\text{DES}) = 3 : 2$; and (D) mixture of $x(\text{TBC}):y(\text{DES}) = 3 : 1$.

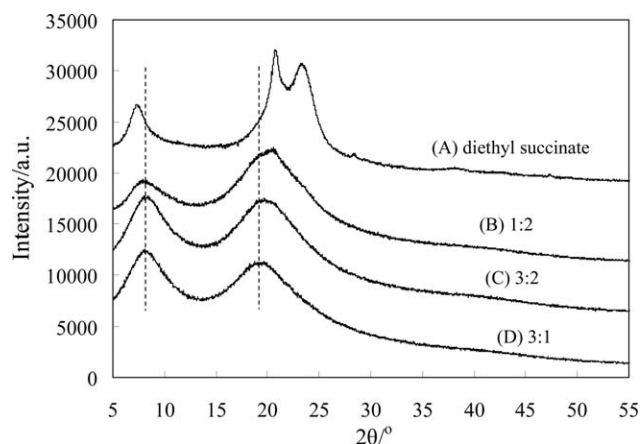


Figure 2. X-ray diffraction diagrams of polymers formed between HMDA and different esters: (A) pure DES; (B) mixture of $x(\text{TBC}):y(\text{DES}) = 1 : 2$; (C) mixture of $x(\text{TBC}):y(\text{DES}) = 3 : 2$; and (D) mixture of $x(\text{TBC}):y(\text{DES}) = 3 : 1$.

(or Pb^{2+} ions) in the solution were determined using a Ca^{2+} ion electrode (or Pb^{2+} ion electrode) (Shanghai Precision & Scientific Instrument) and an ion meter (Shanghai Precision & Scientific Instrument, Model PXB 720A). The chelated metal amount was calculated by subtracting the free metal amount from the initial total amount of the metal. The metal concentrations were found by comparison with standard log $[\text{M}^{2+}]$ versus millivolt plots.

Antifreeze activities were evaluated by their thermal behavior during the thawing of the frozen solutions of the materials, according to the method reported by Mitsuiki.¹⁹ Briefly, 5% (w/w) aqueous solutions of each material, of which the concentration was accurately known, and pure water were used for the measurements of the antifreeze activities. The solutions and pure water (ca. 15 mg) were sealed in aluminum pans, respectively, and accurately weighed. In the DSC measurement, each sample was scanned from -22 to $+30^\circ\text{C}$ at 3°C min^{-1} , after cooling to -22°C at 5°C min^{-1} and holding at -22°C for 10 min. The antifreeze activity (AF) of each

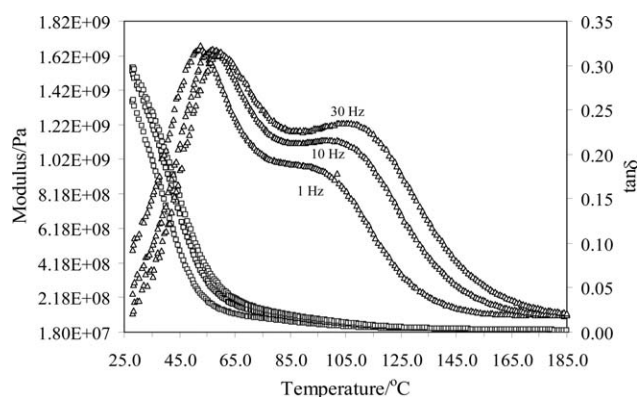


Figure 3. Dynamic mechanical analysis results of the copolymer film prepared with $x(\text{TBC}):y(\text{DES}) = 1 : 2$ at a frequency of 1, 10, and 30 Hz. The storage modulus and loss tangent curves are shown as hollow squares and triangles, respectively.

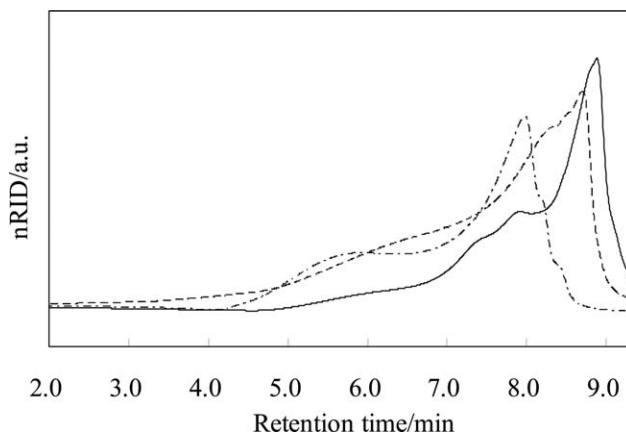


Figure 4. GPC retention profiles of hydrolyzed products prepared from a mixture of $x(\text{TBC}):y(\text{DES}) = 1 : 2$ (solid line); $3 : 2$ (dashed line); and $3 : 1$ (dash-dotted line).

sample was defined as the grams of unfrozen water in its solution per gram of the solid sample and was calculated using eq. (1),¹⁹

$$\begin{aligned} \text{AF} &= (\text{unfrozen water}) / (\text{solid sample}) \\ &= \{ [\Delta H_{\text{water}}(1-w) - \Delta H_A](1-w) / [\Delta H_{\text{water}}(1-w)] \} / w \\ &= [\Delta H_{\text{water}}(1-w) - \Delta H_A] / (\Delta H_{\text{water}} w) \end{aligned} \quad (1)$$

where w is the weight fraction of the sample in the solution, ΔH_A and ΔH_{water} is the heat of fusion of a sample solution and pure water, respectively.

RESULTS AND DISCUSSION

Formation of Poly(succinamide-co-succinamide) Polymers based on Succinic Acid and Citric Acid

The polymerization reactions used in the present study are shown in Scheme 2. Diethyl succinate (DES) and tributyl citrate (TBC) were prepolymerized with hexamethylenediamine (HMDA) at 70°C , resulting in amide linkages (Structure 1 in Scheme 2) after elimination of the ethyl alcohol and butyl alcohol. Continuous heating at 160°C for 4 h, and then at 200°C for 4 h led to formation of solid films with imide rings (Structure 2 in Scheme 2).

Because of the presence of the trifunctional monomer TBC, the resulting polymers can possess a branched structure (see

Table II. Molecular Weights (M_n and M_w) of Succinamide-Citramide Copolymers

Ratio of $x(\text{TBC}):y(\text{DES})$	1 : 2	3 : 2	3 : 1
Retention volumes of eluting peaks (mL)	8.88	8.69	7.97
M_n	4.89×10^3	1.31×10^4	6.20×10^4
M_w	2.56×10^5	2.29×10^6	4.79×10^6

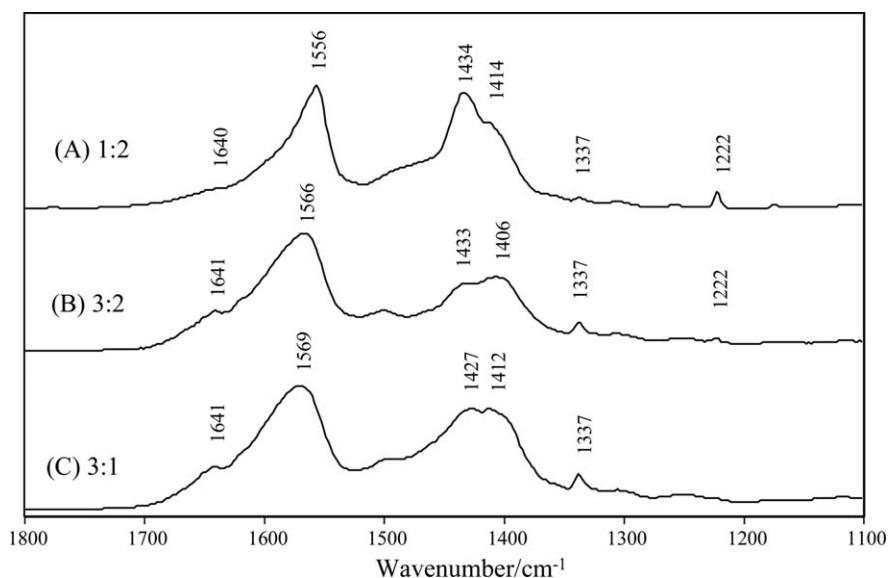


Figure 5. FTIR spectra of hydrolyzed polymers formed between HMDA and different esters: (A) mixture of $x(\text{TBC}):y(\text{DES}) = 1 : 2$; (B) mixture of $x(\text{TBC}):y(\text{DES}) = 3 : 2$; and (C) mixture of $x(\text{TBC}):y(\text{DES}) = 3 : 1$.

Scheme 3). According to Flory's theory, the critical extent of reaction (p_c) of different samples for the gel point can be calculated by eq. (2)

$$p_c = \frac{1}{[r + r\rho(f-2)]^{1/2}} \quad (2)$$

where r is the ratio of the amino group and ester group, ρ is the molar fraction of the ester group from the branching unit TBC in the total ester group in both TBC and DES, f is the functionality of TBC ($f = 3$). The calculation results (Table I) indicate that gel formation can occur in the polymerization process. The higher the TBC content, the easier the gel formation. This was verified by the observation that the reaction mixtures cast in TEFLON molds formed white insoluble gel films in 24 h.

It is noteworthy that formation of Structure 2 (Scheme 2) occurs simultaneously during the polymerization. Figure 1(B–D) illustrate FTIR spectra of the post-polymerized solid films prepared from $x(\text{TBC}):y(\text{DES}) = 1 : 2, 3 : 2, 3 : 1$, respectively. For comparison, FTIR spectrum of polyamides formed by equimolar amount of DES and HMDA in the absence of TBC is displayed in Figure 1(A). The amide I, II, and III vibrational modes are observed at 1632, 1540, and 1256 cm^{-1} , respectively, in Figure 1(A). The strong amide I and amide II bands are clearly observed at 1647 and 1542 cm^{-1} in the polymers formed between HMDA and various mixtures of DES and TBC in Figure 1(B–D). Two new bands at 1773 and 1698 cm^{-1} in Figure 1(B–D) are attributed to in-phase and out-of-phase stretching mode of the two C=O groups in the imide ring, formed from the citrate moiety.^{34,35} Our quantum mechanical calculations of the vibrational normal modes of the succinimide ring have confirmed the assignments of the imide bands at 1773 and 1698 cm^{-1} .³⁵ The upward shift of the amide I band at 1647 cm^{-1} in the copolymers indicates the hydrogen bonding interactions occurring in the amide

linkages become weaker, when compared with the interactions in the pure poly(succinamide) formed between DES and HMDA, most likely due to the disruption of such H-bonding in the presence of the imide rings.³⁶ The FTIR spectra in Figure 1 are consistent with the formation of Structure 2 in Scheme 2.

To examine the effect of imide rings on the crystallinity, X-ray diffraction analysis was performed for the obtained polymers. As shown in Figure 2(A), the pure poly(succinamide) sample displays three relatively sharp peaks at $2\theta = 7.3^\circ, 20.8^\circ,$ and 23.4° , whereas the copolymers only demonstrate two broad peaks at $2\theta = 8.6^\circ$ and 19.8° on the top of the amorphous background in Figure 2(B–D), indicating significant disruption of the potential to form highly ordered lamellar structures in the copolymers. Therefore, the obtained amide-imide copolymers are mainly composed of amorphous structures, unlike the pure poly(succinamide).

Dynamic mechanical analysis was performed for the copolymer films. The $\tan \delta$ curves in Figure 3 show that the sample prepared with $x(\text{TBC}):y(\text{DES}) = 1 : 2$ has two glass transition temperatures, one at 51.9, 57.7, and 60.7°C, while the other appearing at 96.1, 105.2, and 109.8°C, when measured at a frequency of 1, 10, and 30 Hz, respectively. The higher T_g transition can be attributed to the chain segments with the rigid imide rings, while the lower one can be ascribed to the polyamide segments free from the imide rings.

Hydrolysis of Poly(succinamide-co-succimide) Intermediate to Water Soluble Polyamides

The imide ring structures are hydrolyzable in alkaline conditions. As shown in Scheme 2, two types of ring scission in Structure 2 in NaOH solutions lead to water soluble products

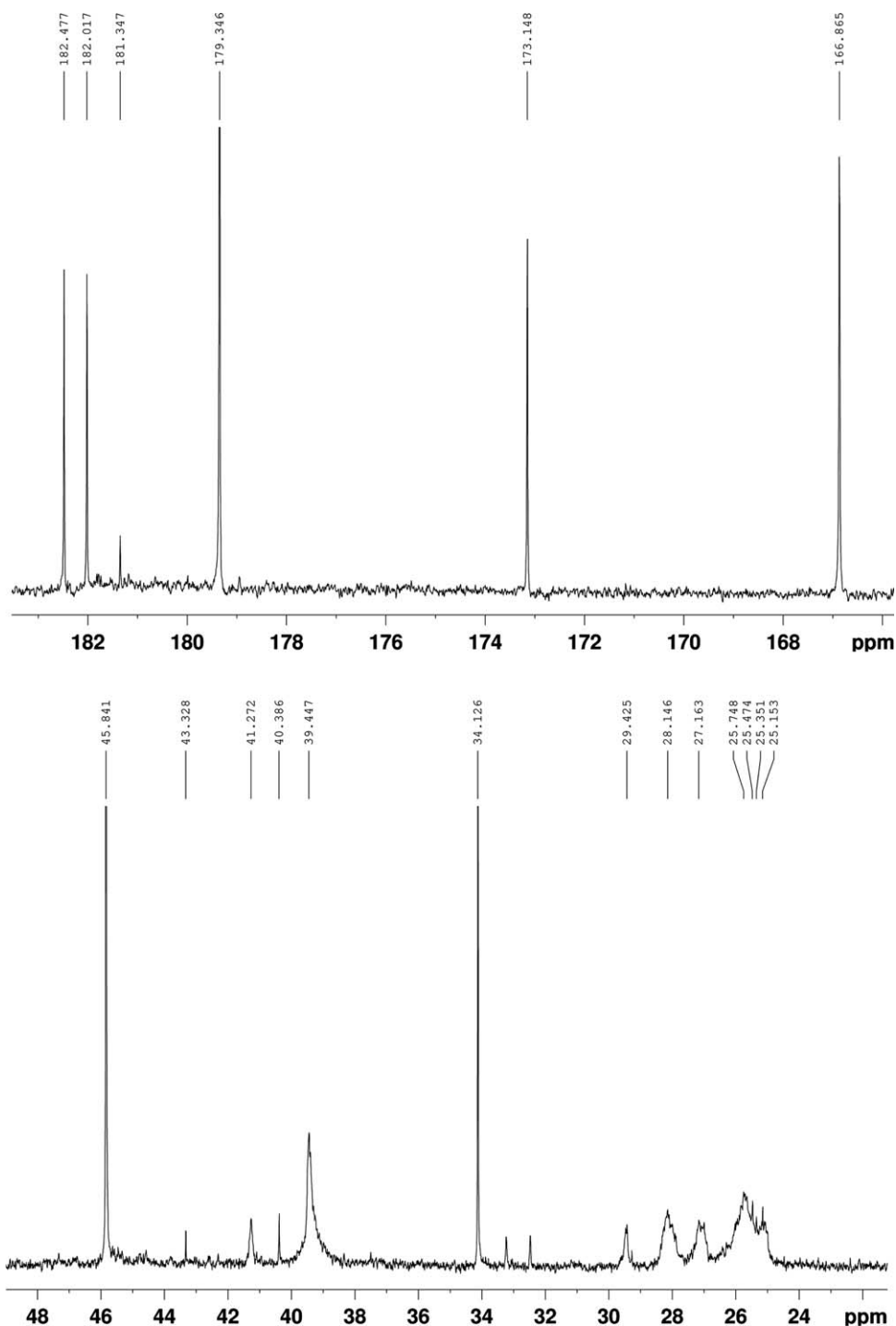


Figure 6. Scale expanded ^{13}C NMR spectrum of the hydrolyzed copolyamide in D_2O with $x(\text{TBC}):y(\text{DES})$ in different chemical shift regions.

(Structure 3 in Scheme 2). GPC analysis of the hydrolyzed products showed that the polymers had M_n ranging from 4.89×10^3 to 6.20×10^4 (Figure 4) (see Table II for the M_n , M_w values). It seems that the molecular weights of the hydrolyzed products increase moderately with increasing amount of TBC used. The broad chromatograms in Figure 4 imply the difficulty in separation of the branched structures with different hydrodynamic radii.

FTIR spectra of the hydrolyzed polymers show very intense bands at $1556\text{--}1569\text{ cm}^{-1}$ and at $1434\text{--}1414\text{ cm}^{-1}$ associated with the carboxylate side chains (Figure 5). The amide I band for the main chain amide groups are seen as a weak shoulder at 1641 cm^{-1} .

NMR spectra were obtained for the hydrolyzed products with $x(\text{TBC}):y(\text{DES}) = 3 : 1$. Ring scission of the imide group in

Table III. Assignments of Carbon Peaks in ^{13}C NMR Spectrum

^{13}C chemical shift (ppm)	Assignment	^{13}C chemical shift (ppm)	Assignment
182.48	side chain COONa in j subunit	45.84	C_2 and C_4
182.02	side chain COONa in k subunit	42–38	αC
179.35	amide C_1 and C_4 in γ subunit	34.13	C_2 and C_3 in γ subunit
173.15	main chain amide C_1 and C_5 in j subunit	30.0–27.0	βC
166.87	main chain amide C_1 and C_6 in k subunit	27.0–25.0	γC
75.20	C_3 in j and k subunit		

Note: see carbon atom labeling in Scheme 4.

Structure 2 led to two types of repeating units (j and k) in Structure 3 (see Scheme 2). In the ^{13}C spectrum shown in Figure 6, the peaks at 182.48 and 182.02 ppm correspond to the resonances in the carbon atoms in the carboxylate side chains of the citrate unit in the j and k repeating units (Table III lists assignment for the ^{13}C peaks; the carbon atom labeling in the hydrolyzed products are shown in Scheme 4). The peak at 179.35 ppm is attributed to the $\text{C}=\text{O}$ carbon atoms in the succinamide in the γ repeating units. The resonances at 173.15 and 166.87 ppm are due to $\text{C}=\text{O}$ carbon atoms in the citramide in the j and k repeating units. The 45.84 ppm peak is due to the methylene carbons in the citramide moiety (C_2 and C_4), while the 34.13 ppm peak is attributed to the methylene carbons in the succinamide moiety (C_2 and C_3). The peaks between 42 and 38 ppm correspond to the αC atoms in the HMDA moiety, and those between 30 and 27 ppm to the βC atoms, while those between 27 and 25 ppm to the γC atoms in

the diamine moiety. The ^{13}C NMR spectrum in Figure 6 confirmed that the obtained product is consistent with Structure 3 in Scheme 2.

The ^1H NMR spectrum in Figure 7 indicates that the protons in the αC atoms in the hexamethylene diamine moiety display two broad peaks between 3.0 and 2.5 ppm. The protons in the methylene groups in the citramide moiety are observed between 2.35 and 2.10 ppm; those in the methylene groups in the succinamide moiety are observed at 2.02 ppm, those in the βC in the HMDA moiety are observed between 1.3 and 1.1 ppm, while those in the γC are observed at 0.94 ppm.

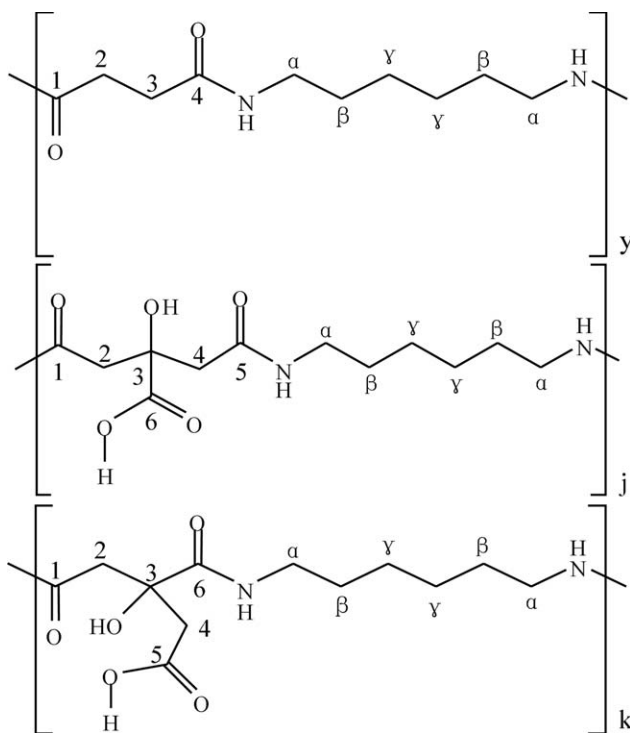
Two dimensional ^{13}C - ^1H HSQC spectrum further verified the above assignments. As shown in Figure 8, the protons appearing between 3.0 and 2.5 ppm are connected to the carbon atoms between 41.27 and 39.45 ppm. The protons between 2.35 and 2.10 ppm are attached to the carbons at 45.84 ppm. The protons at 2.02 ppm are connected to the carbons at 34.13 ppm. The protons between 1.3 and 1.1 ppm are connected to the carbons between 30.0 and 27.2 ppm, while the protons appearing at 0.94 ppm are attached to the carbons appearing between 27.2 and 25.0 ppm.

Metal Chelation

The above NMR study illustrates that the hydrolyzed polyamides and PASP have similarity in their structures; therefore, their metal chelating abilities are examined in this study. As a comparison, PASP is found to have a chelating capability of 180.69 mg g^{-1} toward Ca^{2+} ion and 959.26 mg g^{-1} toward Pb^{2+} ion. The copolyamides prepared with a mixture of $x(\text{TBC}):y(\text{DES}) = 3 : 1$ or $3 : 2$ are found to have similarly high chelating capabilities toward the Ca^{2+} ion (ca. 190 mg g^{-1}) and Pb^{2+} ion (ca. 1000 mg g^{-1}) (Table IV). Hence, the polyamides can use the lone pair electrons in the O atoms of the carboxylic side chains and those in the N and O atoms of backbone amide groups to bind the metals. The nearly same atomic mass ratio $\text{Pb}/\text{Ca} \approx 5.2$ indicates that the chelating ability of the polyamides toward Pd remains approximately five times that toward Ca, on a mass basis, regardless of the polyamide compositions.

Antifreeze Activities

Antifreeze activities of various polyamides obtained were studied by DSC analysis. Figure 9 shows DSC thermograms of the



Scheme 4. Carbon atom labeling in the hydrolyzed products.

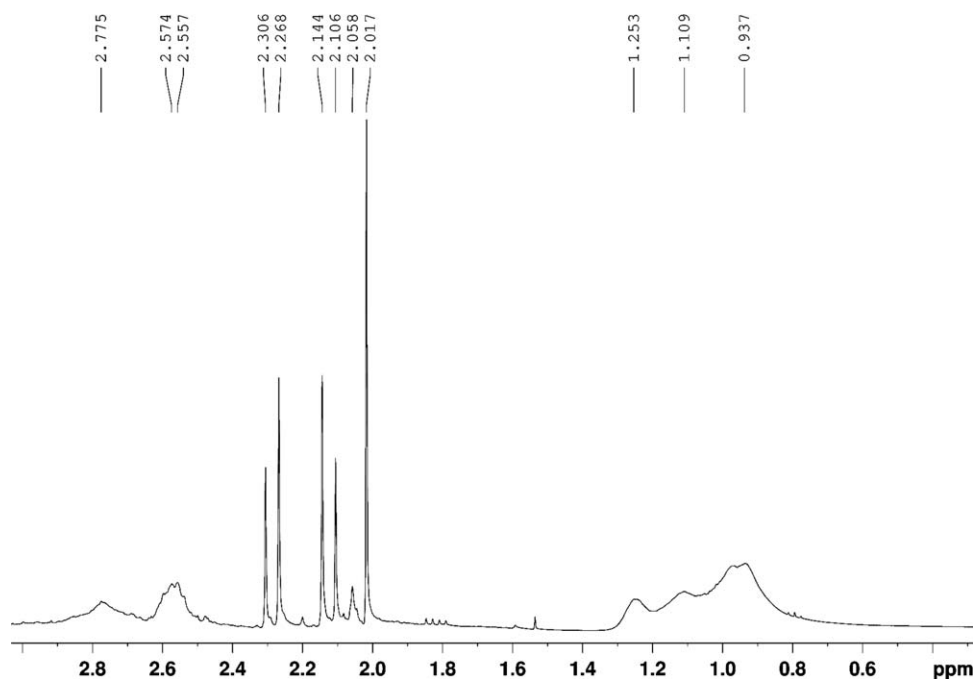


Figure 7. ^1H NMR spectrum of hydrolyzed copolymer in D_2O with $x(\text{TBC}):y(\text{DES}) = 3 : 1$.

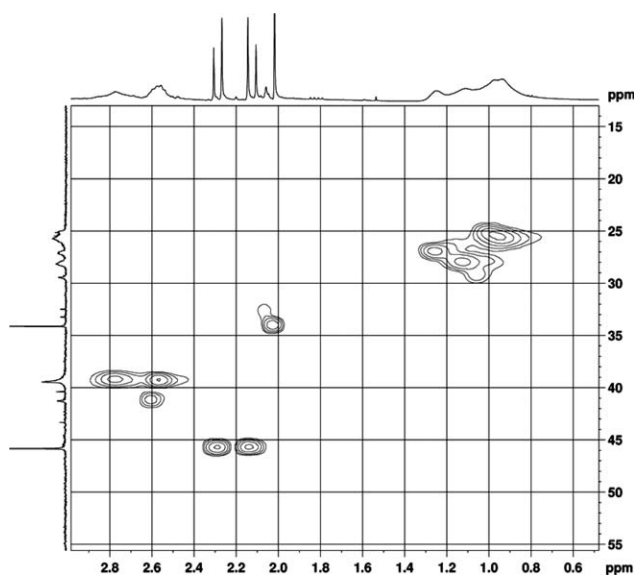


Figure 8. ^{13}C - ^1H HSQC NMR spectrum of the hydrolyzed copolyamide in D_2O with $x(\text{TBC}):y(\text{DES}) = 3 : 1$.

aqueous solutions of the copolyamides and glucose, a well known antifreeze substance, during the thawing of the frozen solutions of the samples. The integrated endothermic peak areas are used to measure the heat of fusion of a sample solution. The antifreeze activity (AF) of each sample characterizes the grams of unfrozen water in its solution per gram of the solid sample and was calculated using the above eq. (1) (see Experimental). Glucose and PASP have an antifreeze activity of 1.09 and 1.18 g of $\text{H}_2\text{O}/\text{g}$, respectively.¹⁹ In Table IV, the calculated antifreeze activity of the copolyamide prepared with a mixture of $x(\text{TBC}):y(\text{DES}) = 3 : 1$ is higher than that of the other two polymers, and much higher than that of glucose or PASP. The DSC data confirm that the depression of both the freezing point and the ice fraction of these frozen water occur when these polymers are added, due to inhibition of crystal growth. This can be understood from the polymer structures that contain hydrophilic $-\text{OH}$ and $-\text{COOH}$ groups for ice binding, and a hydrophobic hexamethylene segment, which renders the addition of further H_2O molecules energetically unfavorable.

CONCLUSIONS

Polyamides formed from diethyl succinate and hexamethylenediamine (nylon 6,4) can become water soluble once tributyl

Table IV. Metal Chelating and Antifreeze Activities of Various Polyamides

Sample	$x(\text{TBC}) : y(\text{DES}) = 1 : 2$	$x(\text{TBC}) : y(\text{DES}) = 3 : 2$	$x(\text{TBC}) : y(\text{DES}) = 3 : 1$
Ca^{2+} (mg g^{-1}) chelation	163.75	190.84	188.59
Pb^{2+} (mg g^{-1}) chelation	877.97	1005.83	996.15
Antifreeze activity ($\text{g of H}_2\text{O}/\text{g}$)	1.42	1.57	3.22

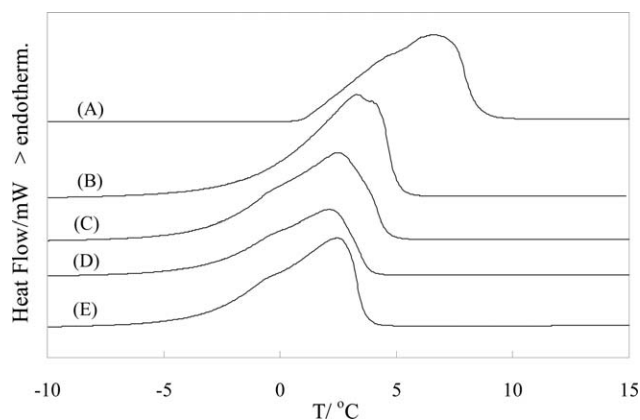


Figure 9. DSC curves of aqueous solutions of different samples: (A) pure water; (B) glucose solution; (C) copolyamide prepared with a mixture of $x(\text{TBC}):y(\text{DES}) = 1 : 2$; (D) copolyamide with $x(\text{TBC}):y(\text{DES}) = 3 : 2$; (E) copolyamide with $x(\text{TBC}):y(\text{DES}) = 3 : 1$.

citrate is copolymerized into the main chain and an alkaline hydrolysis is used for the intermediate copolymers formed. The hydrolyzed copolymers of succinamide and citramide are good metal chelators and expected to be useful for mineralization control in industry or biomimetic modulation of mineral deposition. They also show antifreeze activities in water, in resemblance to the well-known antifreeze substance glucose or synthetic polypeptide poly(aspartic acid), as well as natural antifreeze proteins. However, isolation of large quantities of antifreeze proteins from natural sources such as fish, insects, plants, fungi or bacteria, is prohibitively expensive. In oil and gas industry, the expensive fish antifreeze proteins can act as hydrate crystal inhibitors with attractive biodegradability for use in regions where high biodegradability of oilfield chemicals is preferred due to environmental concerns.^{37–39} The present synthetic process could allow for large scale manufacture of eco-friendly metal chelation polymers and antifreeze polyamides at a low cost, and even at a lower cost than that based on synthesis of poly(amino acid)s.

ACKNOWLEDGMENTS

This was supported by grants from National Natural Science Foundation of China (No: 20974063), Department of Science and Technology of Zhejiang Province (No: 2012C24003), and Natural Science Foundation of Zhejiang Province (No: Y4090504 and LY12E03001).

REFERENCES

- Huang, M. L.; Ehre, D.; Jiang, Q.; Hu, C.; Kirshenbaum, K.; Ward, M. D. *Proc Natl Acad Sci USA* **2012**, *109*, 19922.
- Gibson, M. I.; Barker, C. A.; Spain, S. G.; Albertin, L.; Cameron, N. R. *Biomacromolecules* **2009**, *10*, 328.
- Rivas, B. L.; Pereira, E. D.; Palencia, M.; Sánchez, J. *Prog. Polym. Sci.* **2011**, *36*, 294.

- Scholl, M.; Kadlecova, Z.; Klok, H.-A. *Prog. Polym. Sci.* **2009**, *34*, 24.
- Endo, K.; Ito, Y.; Higashihara, T.; Ueda, M. *Eur. Polym. J.* **2009**, *45*, 1994.
- Itaka, K.; Ishii, T.; Hasegawa, Y.; Kataoka, K. *Biomaterials* **2010**, *31*, 3707.
- Peng, S.-F.; Yang, M.-J.; Su, C.-J.; Chen, H.-L.; Lee, P.-W.; Wea, M.-C.; Sung, H.-W. *Biomaterials* **2009**, *30*, 1797.
- Petersen, H.; Merdan, T.; Kunath, K.; Fischer, D.; Kissel, T. *Bioconj. Chem.* **2002**, *13*, 812.
- Pattabiraman, V. R.; Bode, J. W. *Nature* **2011**, *480*, 471.
- Okamura, A.; Hirai, T.; Tanihara, M.; Yamaoka, T. *Polymer* **2002**, *43*, 3549.
- Tachibana, Y.; Kurisawa, M.; Uyama, H.; Kakuchi, T.; Kobayashi, S. *Chem. Commun.* **2003**, 106.
- Yamazaki, N.; Higashi, F.; Kawabata, J. *J. Polym. Sci. Polym. Chem. Ed.* **1974**, *12*, 2149.
- Neuse, E. W.; Perlwitz, A. G.; Schmitt, S. *Angew. Makromol. Chem.* **1991**, *192*, 35.
- Regano, C.; Alla, A.; De Ilarduya, A. M.; Munoz-Guerra, S. *J. Polym. Sci. A Polym. Chem.* **2004**, *42*, 1566.
- Majo, M. A.; Alla, A.; Bou, J. J.; Herranz, C.; Munoz-Guerra, S. *Eur. Polym. J.* **2004**, *40*, 2699.
- de G. Garcia-Martin, M.; Hernandez, E. B.; Perez, R. R.; Alla, A.; Munoz-Guerra, S.; Galbis, J. A. *Macromolecules* **2004**, *37*, 5550.
- Esquivel, D.; Bou, J. J.; Munoz-Guerra, S. *Polymer* **2003**, *44*, 6169.
- Kiely, D. E.; Chen, L.; Lin, T.-H. *J. Am. Chem. Soc.* **1994**, *116*, 511.
- Mitsuiki, M.; Mizuno, A.; Tanimoto, H.; Motoki, M. *J. Agric. Food. Chem.* **1998**, *46*, 891.
- Kubota, H.; Matsunobu, T.; Uotani, K.; Takebe, H.; Satoh, A.; Tanaka, T.; Taniguchi, M. *Biosci. Biotech. Biochem.* **1993**, *57*, 1212.
- Cheng, H. N. In *Enzyme-Catalyzed Synthesis of Polyamides and Polypeptides, Biocatalysis in Polymer Chemistry*; Loos, K., Ed.; Wiley-VCH Verlag GmbH & Co. KGaA: Weinheim, Germany, **2010**, 131.
- Yagci, Y. E.; Antonietti, M.; Borner, H. G. *Macromol. Rapid. Commun.* **2006**, *27*, 1660.
- Kelland, M. A.; Villano, L. D.; Kommedal, R. *Energy Fuels* **2008**, *22*, 3143.
- Lunde, A.; Sabo, M.; Kelland, M. A. Dual Kinetic Hydrate Inhibition and Scale Inhibition by Polyaspartamides, Proceedings of 7th International Conference on Gas Hydrates (ICGH7), Edinburgh, July 2011.
- Hasson, D.; Shemer, H.; Sher, A. *Ind. Eng. Chem. Res.* **2011**, *50*, 7601.
- Kelland, M. A. In *Advances in Materials Science Research*; Wythers, M. C., Ed.; Nova Science, **2012**; Vol. 8, Hauppauge, NY, USA, Chapter 5, p. 171.

27. Villano, L. D.; Kommedal, R.; Kelland, M. A. Proceedings of the 6th International Conference on Gas Hydrates (ICGH6), Vancouver, Canada, July, **2008**.
28. Bechthold, I.; Bretz, K.; Kabasci, S.; Kopitzky, R.; Springer, A. *Chem. Eng. Technol.* **2008**, *31*, 647.
29. Kabasci, S.; Bretz, I. In *Renewable Polymers: Synthesis, Processing, and Technology*; Mittal, V., Ed.; Wiley: Hoboken, New Jersey, **2011**; Chapter 8. 355.
30. Berovic, M.; Legisa, M. *Biotechnol. Annu. Rev.* **2007**, *13*, 303.
31. Nakato, T.; Yoshitake, M.; Matsubara, K.; Tomida, M.; Kakuchi, T. *Macromolecules* **1998**, *31*, 2107.
32. Doll, K. M.; Shogren, R. L.; Willett, J. L.; Swift, G. J. *Polym. Sci. A Polym. Chem.* **2006**, *44*, 4259.
33. Okada, Y.; Banno, T.; Yoshima, K.; Matsumura, S. *J. Oleo. Sci.* **2009**, *58*, 519.
34. Couffin-Hoarau, A.-C.; Boustta, M.; Vert, M. *J. Polym. Sci. A Polym. Chem.* **2001**, *39*, 3475.
35. Zhu, X.; Lu, P.; Chen, W.; Dong, J. *Polymer* **2010**, *51*, 3054.
36. Painter, P. C.; Coleman, M. *Fundamentals of Polymer Science*, 2nd Ed.; Technomic Publishing: Lancaster, PA, USA, **1997**.
37. Zeng, H.; Wilson, L. D.; Walker, V. K.; Ripmeester, J. A. *J. Am. Chem. Soc.* **2006**, *128*, 2844.
38. Zeng, H.; Moudrakovski, I. L.; Ripmeester, J. A.; Walker, V. K. *AIChE J.* **2006**, *52*, 3304.
39. Ohno, H.; Susilo, R.; Gordienko, R.; Ripmeester, J.; Walker, V. K. *Chem. Eur. J.* **2010**, *16*, 10409.